Inorganic Chemistry
Article

Inorg. Chem. **2010**, *49*, 2457–2463 **2457**
DOI: 10.1021/ic9023184

Lanthanide Complexes of Boraamidinate Ligands: Synthesis and X-ray Structures of $\{[Li(THF)_4][\textit{bam}LnCl_2(THF)]\}_2$ (*bam* = $[PhB(NDipp)_2]^{2-}$; Ln = Y, Pr, Nd, Sm, Ho, Er, Yb) and $\{\textit{bam}LnCl(THF)_2\}_2$ (Ln = Y, Sm)

Andrea M. Corrente and Tristram Chivers*

Department of Chemistry, University of Calgary, Calgary, Alberta T2N 1N4, Canada

Received November 23, 2009

The first examples of the incorporation of the boraamidinate ligand into lanthanide complexes have been prepared by reaction of equimolar amounts of $[Li_2][PhB(NDipp)_2]$ and $LnCl_3$ in tetrahydrofuran (THF), which produces "ate" complexes of the form $\{[Li(THF)_4][\textit{bam}LnCl_2(THF)]\}_2$ [Ln = Y (**9a**), Pr (**9b**), Nd (**9c**), Sm (**9d**), Ho (**9e**), Er (**9f**), Yb (**9g**)] through the inclusion of the LiCl by-product. The isostructural complexes **9a**−**g** were characterized in the solid state by X-ray crystallography, which revealed ion-separated complexes composed of a dimeric anion with a terminal and a bridging chloride ligand on each metal center and a tetrasolvated cation, $[Li(THF)_4]^+$. In solution, the yttrium complex **9a** was characterized by multinuclear (^1H, ^{13}C, ^7Li, and ^{11}B) NMR spectroscopy. The ^1H and ^7Li NMR spectra of the paramagnetic complexes **9b**−**9d** showed broad resonances, but NMR spectra could not be obtained for **9e**−**g**. The complexes **9a**−**g** are readily soluble in THF, but insoluble in diethyl ether and hexane. The reaction of $\{[Li(THF)_4][\textit{bam}LnCl_2(THF)]\}_2$ (Ln = Y, Sm) with an excess of trimethysilyl trifluoromethanesulfonate (TMSOTf) generates the dimeric neutral complexes $\{\textit{bam}LnCl(THF)_2\}_2$, which have been characterized by ^1H NMR and X-ray crystallography.

Introduction

Boraamidinates,[1] *bams* (**1**), are dianionic ligands isoelectronic to the well-studied amidinates, *ams* (**2a**).[2] The formal replacement of the −CR fragment in *ams* with a −BR unit imparts two significant consequences: fewer ligands are required to charge-balance a metal center and intriguing redox behavior can be observed through one-electron oxidation.[3] The electronic properties of **2a** are altered significantly by changing the alkyl/aryl substituent on carbon to a dialkylamino group, that is, in guanidinates, *guans* (**2b**). For example, the *guan* ligand stabilizes a complex with a magnesium−magnesium bond[4] as well as cobalt(I) complexes.[5] The formal replacement of the alkyl/aryl substituent in *bams* (**1**) by a dialkylamino group generates boraguanidinates, *bogs* (**3**), which exhibit substantially increased reducing power compared to *bams*.[6]

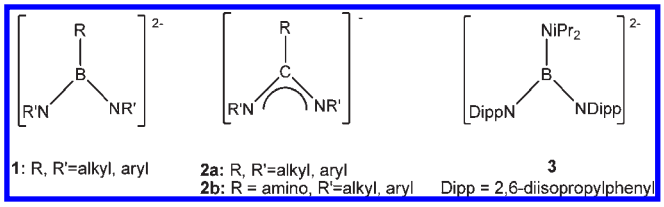

1: R, R'=alkyl, aryl

2a: R, R'=alkyl, aryl
2b: R = amino, R'=alkyl, aryl

3
Dipp = 2,6-diisopropylphenyl

In comparison to the carbon-based ligands, the chemistry of *bams* is less thoroughly investigated. Although *ams* and *guans* are well-known to form complexes with main group and transition metals, as well as with lanthanides and actinides,[2] the scope of the *bam* ligand is limited primarily to main group systems, with relatively few d-block complexes found in the literature.[1] Notably, the chemistry of *bams* with f-block metals remains unexplored. However, numerous other dianionic ligands have been incorporated into lanthanide complexes and structurally characterized, including the following: the cyclooctatetraene dianion,[7a] the

*To whom correspondence should be addressed. E-mail: chivers@ucalgary.ca. Phone: (403) 220-5741. Fax: (403) 289-9488.

(1) For a recent review, see: Fedorchuk, C.; Copsey, M.; Chivers, T. *Coord. Chem. Rev.* **2007**, *251*, 897.
(2) For a recent review on the chemistry of amidinates and guanidinates, see: Edelmann, F. T. *Adv. Organomet. Chem.* **2008**, *57*, 183.
(3) (a) Chivers, T.; Eisler, D. J.; Fedorchuk, C.; Schatte, G.; Tuononen, H. M.; Boeré, R. T. *Chem. Commun.* **2005**, 3930. (b) Chivers, T.; Eisler, D. J.; Fedorchuk, C.; Schatte, G.; Tuononen, H. M.; Boeré, R. T. *Inorg. Chem.* **2006**, *45*, 2119.
(4) Green, S. P.; Jones, C.; Stasch, A. *Science* **2007**, *318*, 1754.
(5) Jones, C.; Schulten, C.; Rose, R. P.; Stasch, A.; Aldridge, S.; Woodul, W. D.; Murray, K. S.; Moubaraki, B.; Brynda, M.; La Macchia, G.; Gagliardi, L. *Angew. Chem., Int. Ed.* **2009**, *48*, 7406.
(6) Corrente, A. M.; Chivers, T. *Inorg. Chem.* **2008**, *47*, 10073.
(7) (a) Hodgson, K. O.; Raymond, K. N. *Inorg. Chem.* **1972**, *11*, 171. (b) Cassani, M. C.; Gun'ko, Y. K.; Hitchcock, P. B.; Lappert, M. F. *Chem. Commun.* **1996**, 1987. (c) Cassani, M. C.; Gun'ko, Y. K.; Hitchcock, P. B.; Lappert, M. F.; Laschi, F. *Organometallics* **1999**, *18*, 5539.

Published on Web 02/01/2010

1,4-cyclohexa-2,5-dienyl (benzene 1,4-dianion) ligand;[7b,c] the antiaromatic 2,2′-bipyridine dianion (bipy^{2-});[8] tetradentate, dianionic Schiff bases;[9] chelating diamides;[10] binaphtholates[11] and bridged cyclopentadienyl ligands.[11] Most recently, lanthanide complexes containing an indenyl-pyrrolyl ligand linked by a methylene spacer (**4**),[12] a β-ketoiminate bearing an *N*-aryloxo substituent (**5**),[13] 1,2-bis[(2,6-diisopropylphenyl)imino]acenaphthene (dpp-Bian) (**6**),[14a,b] derivatives of β-diketiminato with pendant amide donors (**7**),[15] and a bis(amido)cyclodiphospha(III)azane (**8**)[16] have been reported.

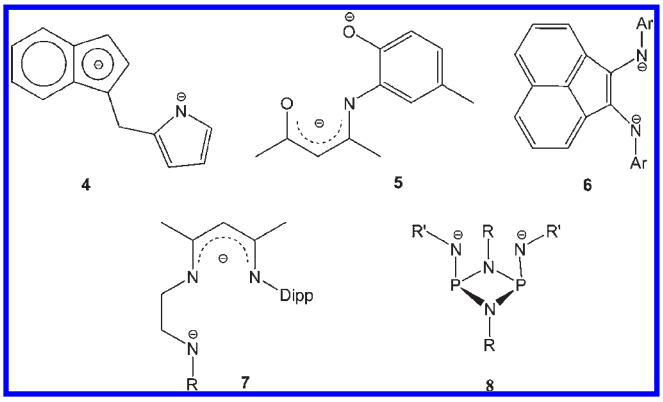

In recent years, there has been growing interest in using amidinate and guanidinate complexes of the lanthanides as catalysts for various processes such as ring-opening polymerization of cyclic esters[17−22] and olefin polymerization.[23,24] Hybrid *bam*/*am* ligands have shown potential as initiators for the polymerization of *rac*-Lactide when incorporated into organomagnesium complexes.[25] Homoleptic guanidinate lanthanide complexes are also being investigated as potential precursors for thin films of rare-earth oxides.[26] It is therefore of interest to pursue analogous lanthanide complexes containing *bams* to examine the effects of the structural and electronic differences introduced by the dianionic ligand. Specifically, the more open coordination environment around the Ln^{3+} center may lead to increased catalytic activity.[27]

Herein we report the synthesis and structural characterization of the dimeric "ate" complexes $\{[Li(THF)_4][bamLnCl_2(THF)]\}_2$ (*bam* = $[PhB(NDipp)_2]^{2-}$; Dipp = 2,6-diisopropylphenyl, Ln = Y (**9a**), Pr (**9b**), Nd (**9c**), Sm (**9d**), Ho (**9e**), Er (**9f**), Yb (**9g**); THF = tetrahydrofuran), the first examples of lanthanide complexes of the boraamidinate ligand,[28] as well as the synthesis and structural characterization of the neutral dimers $\{bamLnCl(THF)_2\}_2$ (Ln = Y (**10a**), Sm (**10d**)) prepared from the reaction of **9a** or **9d** with an excess of TMSOTf. The *N*-Dipp substituted ligand $[PhB(NDipp)_2]^{2-}$ was chosen in preference to the more widely studied *N*-*tert*-butyl analogue $[PhB(N^tBu)_2]^{2-}$ in an effort to provide better steric protection of low-coordinate Ln centers.[1] Metathetical reactions of $\{bamSmCl(THF)_2\}_2$ with lithium or potassium bis(trimethylsilyl)amide and with lithium diisopropylamide have also been investigated.

Experimental Section

Reagents and General Procedures. All reactions and the manipulation of moisture- and/or air-sensitive products were carried out under an atmosphere of argon using standard Schlenk line techniques or in an inert-atmosphere glovebox. Solvents were dried with appropriate drying agents, distilled before use, and stored over molecular sieves. Prior to use, all glassware was carefully dried. The anhydrous reagents $PrCl_3$, $NdCl_3$, $HoCl_3$, $ErCl_3$, and $YbCl_3$ were purchased from Strem, and all other chemicals were purchased from Aldrich Chemical Co. All chemicals were used as received, with the exception of 2,6-diisopropylaniline (97%, Aldrich), which was purified by distillation (at approximately 100 °C and 10^{-2} Torr). The reagent LiN(H)Dipp was prepared by the addition of ^{n}BuLi (2.5 M in hexane) to an equimolar amount of $DippNH_2$ in *n*-hexanes, and purity was checked by ^{1}H NMR spectroscopy. Deuterated solvents were purchased from Cambridge Isotope Laboratories, dried over molecular sieves for at least 1 week and degassed using the freeze−pump−thaw method. Dilithio boraamidinate $[Li_2][PhB(NDipp)_2]$ was prepared by the literature method.[29]

Instrumentation. All NMR spectra were acquired at room temperature using a Bruker DRX 400 spectrometer. All chemical

(8) Fedushkin, I. L.; Petrovskaya, T. V.; Girgsdies, F.; Köhn, R. D.; Bochkarev, M. N.; Schumann, H. *Angew. Chem., Int. Ed.* **1999**, *38*, 2262.
(9) (a) Schuetz, S. A.; Silvernail, C. M.; Incarvito, C. D.; Rheingold, A. L.; Clark, J. L.; Day, V. W.; Belot, J. A. *Inorg. Chem.* **2004**, *43*, 6203. (b) Schuetz, S. A.; Day, V. W.; Rheingold, A. L.; Belot, J. A. *Dalton Trans.* **2003**, 4303. (c) Schuetz, S. A.; Day, V. W.; Clark, J. L.; Belot, J. A. *Inorg. Chem. Commun.* **2002**, *5*, 706. (d) Evans, W. J.; Fujimoto, C. H.; Ziller, J. W. *Polyhedron* **2002**, *21*, 1683. (e) Schuetz, S. A.; Day, V. W.; Sommer, R. D.; Rheingold, A. L.; Belot, J. A. *Inorg. Chem.* **2001**, *40*, 5292. (f) Evans, W. J.; Fujimoto, C. H.; Ziller, J. W. *Chem. Commun.* **1999**, 311. (g) Liu, Q.; Ding, M. *J. Organomet. Chem.* **1998**, *553*, 179. (h) Liu, Q.; Ding, M.; Lin, Y.; Xing, Y. *Polyhedron* **1998**, *17*, 2327. (i) Liu, Q.; Ding, M.; Lin, Y.; Xing, Y. *Polyhedron* **1998**, *17*, 555. (j) Dubé, T.; Gambarotta, S.; Yap, G. *Organometallics* **1998**, *17*, 3967. (k) Liu, Q.; Ding, M.; Lin, Y.; Xing, Y. *J. Organomet. Chem.* **1997**, *548*, 139.
(10) (a) Li-Ying, Z.; Hong-Ting, S.; Ying-Ming, Y.; Yong, Z.; Qi, S. *J. Organomet. Chem.* **2007**, *692*, 2990. (b) Collin, J.; Daran, J.-C.; Jacquet, O.; Schulz, E.; Trifonov, A. *Chem.—Eur. J.* **2005**, *11*, 3455. (c) Lorenz, V.; Görls, H.; Thiele, S.K.-H.; Scholz, J. *Organometallics* **2005**, *24*, 797. (d) Sugiyama, H.; Korobkov, I.; Gambarotta, S. *Inorg. Chem.* **2004**, *43*, 5771. (e) Roesky, P. W. *Organometallics* **2002**, *21*, 4756.
(11) For a review see: Aspinall, H. C. *Chem. Rev.* **2002**, *102*, 1807.
(12) Pi, C.; Zhang, Z.; Liu, R.; Weng, L.; Chen, Z.; Zhou, X. *Organometallics* **2006**, *25*, 5165.
(13) Peng, H.; Zhang, Z.; Qi, R.; Yao, Y.; Zhang, Y.; Shen, Q.; Cheng, Y. *Inorg. Chem.* **2008**, *47*, 9828.
(14) (a) Fedushkin, I. L.; Maslova, O. V.; Baranov, E. V.; Shavyrin, A. S. *Inorg. Chem.* **2009**, *48*, 2355. (b) Vasudevan, K.; Cowley, A. H. *Chem. Commun.* **2007**, 3464.
(15) Lu, E.; Gan, W.; Chen, Y. *Organometallics* **2009**, *28*, 2318.
(16) Rastätter, M.; Muterle, R. B.; Roesky, P. W.; Thiele, S. K.-H. *Chem.—Eur. J.* **2009**, *15*, 474.
(17) Luo, Y.; Yao, Y.; Shen, Q.; Sun, J.; Weng, L. *J. Organomet. Chem.* **2002**, *662*, 144.
(18) Luo, Y.; Yao, Y.; Shen, Q.; Yu, K.; Weng, L. *Eur. J. Inorg. Chem.* **2002**, 318.
(19) Zhou, L.; Sun, H.; Chen, J.; Yao, Y.; Shen, Q. *J. Polym. Sci., Part A: Polym. Chem.* **2005**, *43*, 1778.
(20) Li, C.; Wang, Y.; Zhou, L.; Sun, H.; Shen, Q. *J. Appl. Polym. Sci.* **2006**, *102*, 22.
(21) Ajellal, N.; Lyubov, D. M.; Sinenkov, M. A.; Fukin, G. K.; Cherkasov, A. V.; Thomas, C. M.; Carpentier, J.-F.; Trifonov, A. A. *Chem.—Eur. J.* **2008**, *14*, 5440.
(22) Stanlake, L. J. E.; Beard, J. D.; Schafer, L. L. *Inorg. Chem.* **2008**, *47*, 8062.
(23) Trifonov, A. A.; Skvortsov, G. G.; Lyubov, D. M.; Skorodumova, N. A.; Fukin, G. K.; Baranov, E. V.; Glushakova, V. N. *Chem.—Eur. J.* **2006**, *12*, 5320.
(24) Yang, Y.; Wang, Q.; Cui, D. *J. Polym. Sci., Part A: Polym. Chem.* **2008**, *46*, 5251.
(25) Chivers, T.; Fedorchuk, C.; Parvez, M. *Organometallics* **2005**, *24*, 580.
(26) Milanov, A. P.; Fischer, R. A.; Devi, A. *Inorg. Chem.* **2008**, *47*, 11405.
(27) For example, see: Dehnicke, K.; Greiner, A. *Angew. Chem., Int. Ed.* **2003**, *42*, 1340.
(28) Prof. Dr. Sjoerd Harder has informed us of his concurrent work on related lanthanide complexes of the boraamidinate ligand $[HB(NDipp)_2]^{2-}$.
(29) Chivers, T.; Fedorchuk, C.; Parvez, M. *Inorg. Chem.* **2004**, *43*, 2643.

shifts are reported in parts per million (ppm) with higher frequency taken as positive. Chemical shifts for ^{1}H and $^{13}C\{^{1}H\}$ NMR spectra are reported with respect to tetramethylsilane and were calibrated based on the signal of the residual solvent peak. A solution of 1.0 M LiCl in D_2O was used as the external standard for ^{7}Li NMR spectra, and $^{11}B\{^{1}H\}$ NMR chemical shifts are reported with respect to a solution of $BF_3 \cdot OEt_2$ in C_6D_6.

Crystal Structure Determinations. Single crystals of **9a**−**g**, **10a**, and **10d** suitable for X-ray analysis were covered with Paratone oil and mounted on a glass fiber in a stream of N_2 at 173 K on a Nonius KappaCCD diffractometer ($Mo_{K\alpha}$ radiation, $\lambda = 0.71073$ Å) using COLLECT (Nonius, B.V. 1998) software. The unit cell parameters were calculated and refined from the full data set. All crystal cell refinement and data reduction was carried out using the Nonius DENZO package. After data reduction, the data were corrected for absorption based on equivalent reflections using SCALEPACK (Nonius, B.V. 1998). The structures were solved by direct methods with the SHELXS-97[30] program package, and refinement was carried out on F^2 against all independent reflections by the full-matrix least-squares method by using the SHELXL-97 program.[31] All non-hydrogen atoms were refined with anisotropic thermal parameters. The hydrogen atoms were calculated geometrically and were riding on their respective atoms. For complexes **10a** and **10d**, electron density in two regions was attributed to a disordered hexane molecule for which no suitable model could be found. These regions of electron density were removed from the reflections data using the program SQUEEZE (PLATON), leaving a total void of 496.2 Å^3 and 509.4 Å^3, respectively.

General Synthetic Procedure for {[Li(THF)$_4$][*bam*LnCl$_2$(THF)]}$_2$ (Ln = Y, Pr, Nd, Sm, Ho, Er, Yb). A solution of $[Li_2][PhB(NDipp)_2]$ in THF (10 mL) was added to a stirred slurry of $LnCl_3$ in THF (10 mL) at −80 °C (Ln = Y, Sm, Ho, Er, Yb) or at room temperature (Ln = Pr, Nd). The reaction was kept cold for approximately 30 min then warmed to room temperature and stirred for an additional 1−2 h (Ln = Y, Sm, Ho, Er, Yb) or heated to 65 °C for 1 h (Ln = Pr, Nd). Volatiles were removed in vacuo, and the reaction mixture was treated with hexane (10 mL) and dried under vacuum. Complex **9a** was additionally washed with diethyl ether (5 mL). NMR data for all complexes were collected using the initially formed product, which contained LiCl. Yields (%) are estimated based on the mass of this product; they were calculated by including the five molecules of coordinated THF in the complexes and assuming the inclusion of an equimolar amount of LiCl or, in the case of **10a** and **10d**, LiOTf. X-ray quality crystals of all complexes were obtained from concentrated THF solutions layered with hexanes at −18 °C. Satisfactory CHN analyses were unable to be obtained for recrystallized samples; however, the ^{1}H NMR spectra of the initially formed bulk samples of **9a**−**d**, **10a**, and **10d**, demonstrate their purity. The reactivity of the complexes toward acetonitrile precluded the determination of electrospray ionization mass spectra.

9a: YCl_3 (0.100 g, 0.512 mmol), $[Li_2][PhB(NDipp)_2]$ (0.231 g, 0.511 mmol); Yield: 0.384 g pale yellow powder (75%). ^{1}H NMR (THF-d_8, 25 °C): δ 6.87 (2 H, m), 6.73 (4 H, m), 6.61 (1 H, m), 6.55 (2 H, m) 6.47 (2 H, m), 3.98 (4 H, sept, $^{3}J_{H-H} = 6.78$ Hz), 3.61 (m, $-OCH_2CH_2$ of coordinated THF), 1.78 (m, $-OCH_2CH_2$ of coordinated THF), 1.12 (12 H, d, $^{3}J_{H-H} = 6.78$ Hz), 0.71 (12 H, d, $^{3}J_{H-H} = 6.78$ Hz). ^{11}B NMR (THF-d_8, 25 °C): δ 32.6 (br, s). ^{7}Li NMR (THF-d_8, 25 °C): δ 0.11. ^{13}C NMR (THF-d_8, 25 °C): δ 155.3, 151.0, 141.3, 136.3, 126.3, 126.0, 122.6, 117.8, 68.4 ($O-CH_2-CH_2$ of THF), 28.2, 26.5 ($O-CH_2-CH_2$ of THF), 25.6, 24.6, 15.8.

9b: $PrCl_3$ (0.111 g, 0.449 mmol), $[Li_2][PhB(NDipp)_2]$ (0.204 g, 0.451 mmol); Yield: 0.328 g, pale yellow powder (69%). ^{1}H NMR (THF-d_8, 25 °C): δ 12.37 (2 H, br s), 10.95 (1 H, br s), 10.59 (4 H, br s), 8.39 (2 H, s), 7.16−7.11 (2H, br m), 3.61 (m, $-OCH_2CH_2$ of coordinated THF), 1.75 (m, $-OCH_2CH_2$ of coordinated THF), 0.94 (12 H, br s), −2.80 (4 H, br s), −7.99 (12 H, br s). ^{7}Li NMR (THF-d_8, 25 °C): δ −0.43

9c: $NdCl_3$ (0.109 g, 0.435 mmol), $[Li_2][PhB(NDipp)_2]$ (0.198 g, 0.438 mmol); Yield: 0.260 g, green powder (56%). ^{1}H NMR (THF-d_8, 25 °C): δ 11.46 (2 H, br s), 10.25 (1 H, br s), 8.94 (4 H, br s), 7.11 (2 H, br s), 6.34 (2 H, br s), 3.61 (m, $-OCH_2CH_2$ of coordinated THF), 1.75 (m, $-OCH_2CH_2$ of coordinated THF), 1.12 (12 H, br s), −1.32 (4 H, br s), −6.35 (12 H, br s). ^{7}Li NMR (THF-d_8, 25 °C): δ −0.04.

9d: $SmCl_3$ (0.285 g, 1.11 mmol), $[Li_2][PhB(NDipp)_2]$ (0.503 g, 1.11 mmol); Yield: 1.00 g, orange powder (84%). ^{1}H NMR (THF-d_8, 25 °C): δ 8.99 (2 H, d), 7.36−7.27 (3 H, m), 6.63 (2 H, d), 6.54 (4 H, t), 3.63 (m, $-OCH_2CH_2$ of coordinated THF), 1.78 (m, $-OCH_2CH_2$ of coordinated THF), 3.30 (4 H, br, septet), 1.05 (12 H, d, $^{3}J_{H-H} = 6.2$ Hz), −0.06 (12 H, d, $^{3}J_{H-H} = 6.2$ Hz). ^{7}Li NMR (THF-d_8, 25 °C): δ 0.23.

9e: $HoCl_3$ (0.091 g, 0.332 mmol), $[Li_2][PhB(NDipp)_2]$ (0.150 g, 0.332 mmol); Yield: 0.223 g, cream colored powder (61%). NMR spectra were unable to be obtained.

9f: $ErCl_3$ (0.091 g, 0.333 mmol), $[Li_2][PhB(NDipp)_2]$ (0.151 g, 0.334 mmol); Yield: 0.220 g, light pink powder (61%). NMR spectra were unable to be obtained.

9g: $YbCl_3$ (0.105 g, 0.376 mmol), $[Li_2][PhB(NDipp)_2]$ (0.171 g, 0.378 mmol); Yield: 0.280 g, dark red powder (78%). NMR spectra were unable to be obtained.

Preparation of {*bam*YCl(THF)$_2$}$_2$ (10a). A solution of trimethylsilyl triflate (0.092 g, 0.414 mmol) in THF (2 mL) was added to a solution of **9a** (0.198 g, 0.103 mmol) in THF (7 mL). The resulting solution was stirred for 45 min, volatiles were removed in vacuo, and the resulting sticky solid was washed with ca.7 mL of hexane. Removal of volatiles in vacuo gave a colorless solid, which was a mixture of LiOTf and **10a** (0.166 g, 92%). Colorless, X-ray quality crystals of **10a** were grown from a THF solution layered with hexanes. ^{1}H NMR (THF-d_8, 25 °C): δ 6.82−6.52 (11 H, m), 3.84 (4 H, br, sept), 3.62 (m, $-OCH_2CH_2$ of coordinated THF), 1.78 (m, $-OCH_2CH_2$ of coordinated THF), 1.12 (12 H, d, $^{3}J_{H-H} = 6.71$ Hz), 0.72 (12 H, d, $^{3}J_{H-H} = 6.71$ Hz). ^{11}B NMR (THF-d_8, 25 °C): δ 31.8 (br, s).

Preparation of {*bam*SmCl(THF)$_2$}$_2$ (10d). A solution of trimethylsilyl triflate (0.096 g, 0.432 mmol) in THF (2 mL) was added to a solution of **9d** (0.222 g, 0.108 mmol) in THF (7 mL). The resulting orange solution was stirred for 15 min, volatiles were removed in vacuo, and the resulting sticky solid was washed with ca.7 mL of hexane. Removal of volatiles in vacuo gave **10d** as a mixture of an orange solid and colorless LiOTf (0.201 g). Orange, X-ray quality crystals of **10d** were grown from a THF solution layered with hexanes (24% yield). ^{1}H NMR (THF-d_8, 25 °C): δ 8.97 (2 H, m), 7.44−6.74 (9 H, m), 3.04 (4 H, br, sept), 3.62 (m, $-OCH_2CH_2$ of coordinated THF), 1.78 (m, $-OCH_2CH_2$ of coordinated THF), 0.97 (12 H, br, d), 0.03 (12 H, br, d).

Results and Discussion

Synthesis and X-ray Structures of {[Li(THF)$_4$][*bam*LnCl$_2$(THF)]}$_2$. The reaction of Li_2bam[29] with an equimolar amount of $LnCl_3$ (Ln = Y, Sm, Pr, Nd, Ho, Er, Yb) in THF produces the markedly air- and moisture-sensitive lanthanide "ate" complexes **9a**−**g** (eq 1) in yields ranging from 56 to 84%. The complexes are readily soluble in THF, but they are insoluble in Et_2O, hexane, and toluene,

(30) Sheldrick, G. M. *SHELXS-97, Program for refinement of crystal structures*; University of Göttingen: Göttingen, Germany, 1997.

(31) Sheldrick, G. M. *SHELXS-97, Program for refinement of crystal structures*; University of Göttingen: Göttingen, Germany, 1997.

precluding the removal of the by-product LiCl from the bulk solid.

$$LnCl_3 + Li_2bam \xrightarrow[-\ LiCl]{THF,\ -80^{\circ}C} 1/2\ \{[Li(THF)_4][bamLnCl_2(THF)]\}_2 \quad (1)$$

Ln = Y (**9a**), Pr (**9b**), Nd (**9c**), Sm (**9d**), Ho (**9e**), Er (**9f**), Yb (**9g**)

Crystals of all complexes, suitable for X-ray diffraction, were grown from a THF solution layered with *n*-hexane at about −18 °C. In the solid state, complexes **9a**−**g** exist as isostructural, ion-separated complexes in which the anions dimerize via chloride bridges. The lithium cations are solvated by four THF molecules and two additional molecules of this solvent are present in the crystal lattice. A representative molecular structure is shown in Figure 1, and selected bond lengths and angles are presented in Table 2.

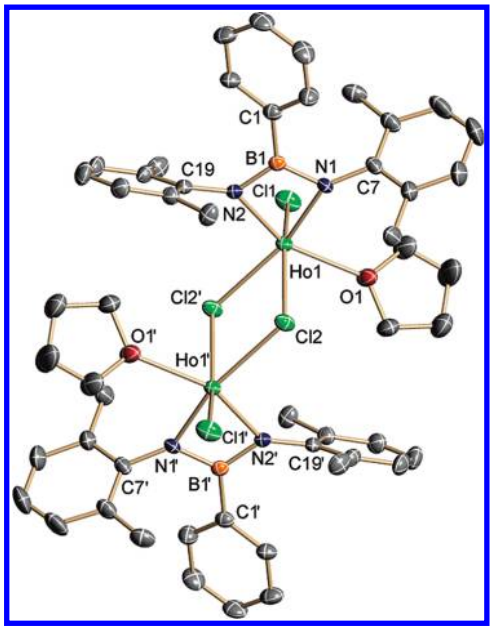

Figure 1. Structure of the anion of **9e**, representative of **9a**−**9g**. Hydrogen atoms, lithium counterions, and lattice solvent (THF) are omitted and only the α-carbon atoms of Dipp groups are shown for clarity. Symmetry elements used to generate equivalent atoms: #1 $-x+2,-y,-z+2$.

In all complexes, the B−N distances are equal within experimental error and have values that are typical for N(2p)→B(2p) π-bonding in boraamidinate complexes.[1] The geometry about boron is planar (the sum of the bond angles is 360°) but is distorted from trigonal, with the N1−B1−N2 angle falling in the range of 112°−114°, while the N1−B1−C1 and N2−B1−C1 bond angles are between 122°−125°. The nitrogen atoms are substantially distorted from a trigonal planar geometry with small B−N−Ln angles of 91°−92° and large C−N−B and C−N−Ln angles in the ranges of about 125°−131° and 135−142°, respectively. The N1−Ln−N2 angle increases going from left to right across the lanthanides series, as a result of the decreasing size of the metal center; this trend holds for complex **9a**, as the radius of yttrium falls between that of holmium and erbium. A search of the Cambridge Structural Database reveals a wide range of Ln−N distances; the values of the Ln−N bonds in **9a**−**g** are at the shorter end of this range, as expected for a chelating dianionic ligand. Indeed, **9a** and **9d**−**f** have comparable Ln−N distances to those reported by Roesky and co-workers who used a dianionic bis(amido)cyclodiphospha(III)azane ligand to form a series of lanthanide complexes, including "ate" complexes with yttrium, samarium, holmium, and erbium.[16] For instance, the Y−N1 and Y−N2 bond lengths of 2.287(5) Å and 2.264(5) Å in the yttrium cyclodiphospha(III)azane "ate" complex[16] are similar to the corresponding distances in **9a** (2.245(3) Å and 2.225(3) Å), but fall on the shorter end of the value expected for an yttrium−nitrogen bond. Similarly, the Ho−N distances of 2.245(3) and 2.223(4) in **9e** are consistent with those in the analogous complex prepared by the Roesky group (2.275(3) Å and 2.263(2) Å),[16] but again are at the lower end of the range of holmium−nitrogen bonds.

For complexes **9a**−**g**, Ln−Cl2 and Ln−Cl2A bond lengths are typical for chlorides bridging the respective lanthanide centers. In all complexes, the chloride bridging is nearly symmetrical, with differences in Ln−Cl2 and Ln−Cl2A lengths ranging from 0.041 Å to 0.056 Å;

Table 1. Crystallographic Data for **9a**−**g**[a,b]

	9a (Y)	9b (Pr)	9c (Nd)	9d (Sm)	9e (Ho)	9f (Er)	9 g (Yb)
fw	1109.92	1161.92	1165.25	1171.36	1185.94	1188.27	1194.05
a, Å	13.385(3)	13.320(3)	13.347(3)	13.356(3)	13.370(3)	13.368(3)	13.394(3)
b, Å	21.503(4)	21.595(4)	21.586(4)	21.563(4)	21.484(4)	21.474(4)	21.458(4)
c, Å	22.053(4)	22.190(4)	22.178(4)	22.123(4)	22.045(4)	22.046(4)	22.062(4)
α, deg.	90	90	90	90	90	90	90
β, deg.	102.88(3)	103.04(3)	103.04(3)	102.99(3)	102.91(3)	102.91(3)	102.86(3)
γ, deg.	90	90	90	90	90	90	90
V, Å^3	6188(2)	6218(2)	6225(2)	6208(2)	6172(2)	6169(2)	6182(2)
μ(Mo Kα), mm^{-1}	1.077	0.917	0.968	1.080	1.417	1.495	1.647
F(000)	2376	2456	2460	2468	2488	2492	2500
Θ range, deg	3.00−25.03	2.75−25.03	3.13−25.03	2.67−25.03	2.68−25.03	2.68−25.03	2.68−25.03
reflns collected	81171	77592	86571	65850	57847	44171	54758
unique reflns	10864	10951	10965	10907	10805	10542	10686
R_{int}	0.0679	0.0477	0.0337	0.0249	0.0350	0.0536	0.0366
R_1 [$I > 2\sigma(I)$][c]	0.0644	0.0620	0.0433	0.0440	0.0445	0.0677	0.0453
wR_2 (all data)[d]	0.1567	0.1296	0.1043	0.1152	0.1155	0.1366	0.1136
GOF on F^2	1.085	1.103	1.059	1.073	1.065	1.124	1.073
completeness	99.4	99.6	99.6	99.4	99.1	96.7	97.9

[a] λ (MoKα) = 0.71073 Å. [b] All structures have the empirical formula $C_{58}H_{95}BCl_2LiN_2O_7Ln$, crystallize in the monoclinic space group $P2(1)/n$ with $Z = 4$, and were collected at −100 °C. [c] $R_1 = \sum||F_o| - |F_c||/\sum|F_o|$. [d] $wR_2 = [\sum w(F_o^2 - F_c^2)^2/\sum wF_o^4]^{1/2}$.

Table 2. Selected Bond Lengths (Å) and Bond Angles (deg) for **9a**−**g**

	9a (Y)	9b (Pr)	9c (Nd)	9d (Sm)	9e (Ho)	9f (Er)	9 g (Yb)
B1−N1	1.435(6)	1.427(7)	1.438(5)	1.440(6)	1.438(6)	1.435(10)	1.447(7)
B1−N2	1.437(6)	1.436(7)	1.451(5)	1.439(6)	1.437(6)	1.448(10)	1.441(7)
N1−Ln	2.245(3)	2.316(4)	2.324(4)	2.297(3)	2.245(3)	2.232(6)	2.208(4)
N2−Ln	2.225(3)	2.335(4)	2.304(3)	2.283(3)	2.223(4)	2.215(6)	2.203(4)
Ln−Cl2	2.717(1)	2.828(2)	2.808(1)	2.779(1)	2.708(1)	2.699(2)	2.686(2)
Ln−Cl2A	2.764(1)	2.871(2)	2.859(1)	2.826(1)	2.761(1)	2.755(2)	2.727(2)
Ln−Cl1	2.602(2)	2.713(2)	2.696(2)	2.665(2)	2.596(2)	2.586(2)	2.572(2)
N1−B1−N2	113.0(4)	113.9(5)	112.6(3)	113.3(4)	112.4(4)	111.9(7)	112.2(5)
N1−B1−C1	123.7(4)	123.8(5)	124.1(3)	123.9(4)	123.9(4)	125.1(7)	124.2(5)
N2−B1−C1	123.3(4)	122.3(5)	123.1(3)	122.8(4)	123.7(4)	123.0(7)	123.6(4)
C7−N1−B1	129.4(3)	130.9(5)	129.8(3)	130.0(4)	129.1(4)	128.5(6)	128.4(4)
C7−N1−Ln	138.1(3)	135.4(3)	136.1(2)	136.6(3)	137.9(3)	138.4(5)	138.8(3)
B1−N1−Ln	90.6(2)	91.6(3)	92.0(2)	91.2(2)	90.9(3)	91.2(4)	90.6(3)
B1−N2−Ln	91.4(2)	92.1(3)	92.5(2)	91.8(2)	91.8(3)	91.6(4)	91.0(3)
C19−N2−B1	125.4(3)	127.5(4)	126.6(3)	127.0(3)	125.8(4)	125.5(6)	125.4(4)
C19−N2−Ln	142.3(3)	139.4(3)	139.8(2)	140.0(3)	141.4(3)	142.1(5)	142.6(3)
N1−Ln−N2	64.8(1)	62.1(1)	62.6(1)	63.3(1)	64.7(1)	65.0(2)	65.8(1)
N1−Ln−O1	88.2(1)	87.1(1)	87.1(1)	87.4(1)	87.9(1)	88.3(2)	88.2(2)
N2−Ln−O1	152.8(1)	148.9(1)	149.4(1)	150.5(1)	152.4(1)	153.1(2)	153.8(2)
N1−Ln−Cl1	100.8(1)	101.4(1)	101.3(1)	101.3(1)	100.7(1)	100.5(2)	100.6(1)
N2−Ln−Cl1	103.1(1)	105.2(1)	104.8(1)	104.3(1)	102.8(1)	102.8(2)	102.4(1)
O1−Ln−Cl1	84.5(1)	83.9(1)	84.0(1)	84.0(1)	84.3(1)	84.3(2)	84.5(1)
N1−Ln−Cl2	99.3(1)	99.8(1)	99.8(1)	99.4(1)	99.5(1)	99.4(2)	99.2(1)
N2−Ln−Cl2	97.4(1)	99.6(1)	99.5(1)	98.9(1)	98.0(1)	97.7(2)	97.1(1)
O1−Ln−Cl2	82.9(1)	80.4(1)	80.7(1)	81.4(1)	82.9(1)	83.1(1)	83.7(1)
Cl1−Ln−Cl2	155.9(1)	152.9(1)	153.2(4)	154.1(1)	155.7(1)	156.0(1)	156.6(1)

overall, these two distances decrease by approximately 0.14 Å from praseodymium to ytterbium. In all cases, the terminal Ln−Cl1 bond lengths are slightly shorter than those typically found in the Cambridge Structural Database and going across the series of lanthanides also decrease by a total of approximately 0.14 Å.

The geometry at the lanthanide center in all complexes is distorted octahedral, with bond angles ranging from approximately 62° to 156°. There is no notable difference in the N1−Ln−Cl angles in **9a**−**f**; however, both N2−Ln−Cl1 and N2−Ln−Cl2 decrease slightly across the series by about 2.8° and 2.5°, respectively. The remaining bond angles about the metal center all increase moving from praseodymium to ytterbium.

NMR Spectra of "ate" Complexes {[Li(THF)$_4$][*bam*LnCl$_2$(THF)]}$_2$. Unlike complexes **9b**−**g**, the yttrium boraamidinate complex **9a** is diamagnetic and easily characterized by multinuclear NMR (^{1}H, ^{7}Li, ^{11}B, ^{13}C). The proton NMR spectrum of **9a** shows the expected multiplets in the aryl region for the phenyl substituent on boron and Dipp groups on nitrogen, which integrate to the appropriate relative intensities, as well as a septet (4 H) and two doublets (12 H), indicative of diastereotopic methyl protons of the Dipp substituents. Multiplets resulting from the THF molecules are also observed at 3.61 ($-OCH_2CH_2$) and 1.78 ($-OCH_2CH_2$) ppm and resonances for residual Et_2O from washing are seen in Figure 2a; the triplet resonance for the Et_2O molecule overlaps with a $-CH(CH_3)_2$ resonance of **9a** at 1.12 ppm, resulting in an integral value larger than the expected 12 H. The ^{7}Li and ^{11}B spectra show singlets at 0.11 and 32.6 ppm, respectively; the former is consistent with a solvated Li^+ cation, while the latter is in the typical range for *bam* complexes.[1]

Despite the paramagnetic nature of complexes **9b**, **9c**, and **9d**, ^{1}H NMR spectra were obtained in a THF-d_8 solution; a summary of chemical shifts is presented in Table 3. As shown in Figure 2, the resonances for the paramagnetic complexes are substantially broadened and in the cases of **9b** and **9c** there is no resolvable ^{1}H−^{1}H coupling. Additionally, a lanthanide-induced shift[32] of the aryl and alkyl protons is observed, with the former resonances being deshielded while the latter are shielded. When compared to the diamagnetic yttrium complex, the greatest shifts are observed for the praseodymium and neodymium complexes. The most deshielded aryl resonance differs by about 5.5 and 4.6 ppm, respectively, the methyne protons are shielded by approximately 6.78 ppm in **9b** and 5.3 ppm in **9c**, and one of the methyl resonances is found 8.70 ppm (**9b**) and 7.06 ppm (**9c**) upfield from those in diamagnetic **9a**. In all complexes, integration of the proton NMR spectrum gives values consistent with the solid-state structure: 11 aryl protons, 4 methyne protons, 24 methyl protons (two resonances, 12 H each) and coordinated THF.

The shifts observed for the samarium complex are less pronounced; aryl resonances are deshielded by $\leq$2 ppm while aliphatic protons are shielded by $<$1 ppm. In contrast, NMR spectra were unable to be obtained for complexes **9e**−**g**, as the paramagnetic nature of these samples prevented the instrument from locking. The ^{11}B NMR resonance for the three-coordinate boron in the *bam* ligand is normally quite broad, and attempts to collect ^{11}B spectra for complexes **9b**−**9d** were unsuccessful, likely a result of further broadening caused by the paramagnetic metal center.

Synthesis and X-ray Structures of {*bam*LnCl(THF)$_2$}$_2$. It has been shown that heating lanthanide "ate" complexes containing the dianionic bis(amido)cyclodiphospha(III)azane ligand in toluene forces the elimination of LiCl to generate neutral species.[16] Boraamidinate lanthanide complexes **9a**−**d** display very limited solubility in toluene-d_8, and the ^{1}H NMR spectrum of the solution

(32) Peters, J. A.; Huskens, J.; Raber, D. J. *Prog. Nucl. Magn. Reson. Spectrosc.* **1996**, *28*, 283.

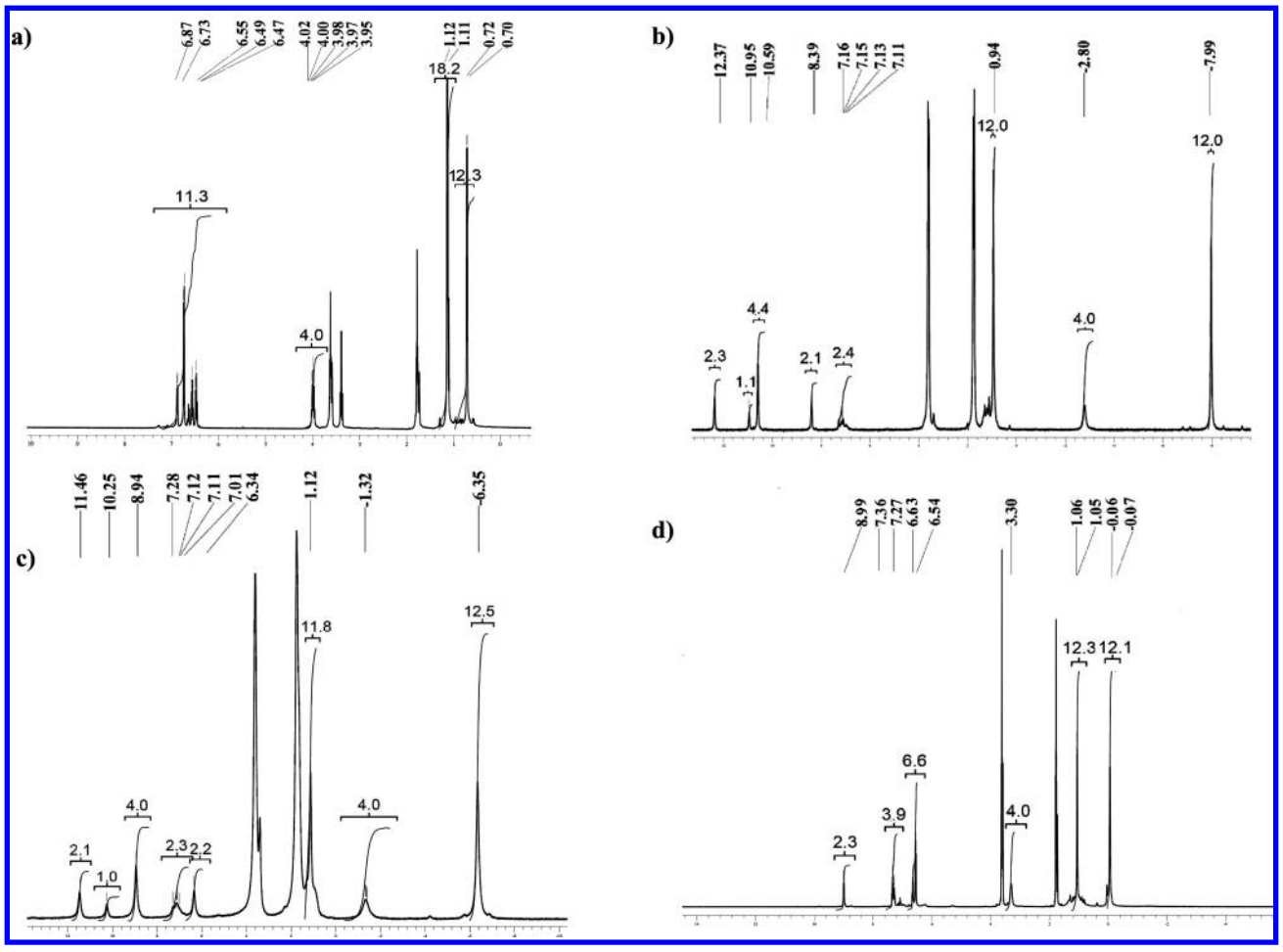

Figure 2. ^{1}H NMR spectra of $\{[Li(THF)_4][bamLnCl_2(THF)]\}_2$ (a) Ln = Y; (b) Ln = Pr; (c) Ln = Nd; (d) Ln = Sm. The unlabeled resonances at about 3.6 and 1.8 in each spectrum are those of the $-OCH_2CH_2$ and $-OCH_2CH_2$ protons, respectively, in the coordinated THF molecules.

Table 3. ^{1}H NMR Chemical Shifts (in ppm) for Complexes **9a**−**d** (in THF-d_8)

	9a (Y)	9b (Pr)	9c (Nd)	9d (Sm)
aryl	6.87, 6.73, 6.61, 6.55, 6.47	12.37, 10.95, 10.59, 8.39, 7.16−7.11	11.46, 10.25, 8.94, 7.11, 6.34	8.99, 7.36, 7.27, 6.63, 6.54
$-CH(CH_3)_2$	3.98	−2.80	−1.32	3.30
$-CH(CH_3)_2$	1.12, 0.71	0.94, −7.99	1.12, −6.35	1.05, −0.06

shows multiple sets of broad resonances that cannot easily be assigned, both at room temperature and after heating. The treatment of **9a** or **9d** with either LiMe or LiHMDS (HMDS = hexamethyldisilylazide) in attempts to generate the alkyl or amide derivatives, respectively, gives complex reaction mixtures. However, the reaction of **9a** or **9d** with an excess of trimethylsilyl trifluoromethanesulfonate (TMSOTf) proceeds cleanly with loss of trimethylsilyl chloride and lithium triflate to give the neutral *bam*LnCl complex (**10a**: Ln = Y, **10d**: Ln = Sm), (eq 2). The formation of **10a** and **10d** does not proceed to completion when a stoichiometric amount of TMSOTf is employed. Trimethylsilyl trifluoromethanesulfonate has been used in metathetical reactions for anion exchange;[33] however, to the best of our knowledge, this is the first example of removal of LiCl by this triflate reagent. Interestingly, the reaction of **9d** with silver trifluoromethanesulfonate (AgOTf) gives multiple products by ^{1}H NMR, none of which are the neutral complex. Colorless and deep orange X-ray quality crystals of **10a** and **10d**, respectively, were grown from a THF solution layered with *n*-hexane. The molecular structure of **10d**, which is also representative of **10a**, is shown in Figure 3, and crystallographic data are summarized in Table 4. Selected bond lengths and bond angles are listed in Table 5.

$$\{[Cl_2Lnbam(THF)][Li(THF)_4]\}_2 + 4\ TMSOTf \xrightarrow[-\ 2\ LiOTf]{-\ 2\ Me_3SiCl} \{bamLnCl(THF)_2\}_2 \quad (2)$$

10a, Ln = Y
10d, Ln = Sm

The values of the B−N distances in both **10a** and **10d** fall in the range expected for N(2p)→B(2p) π-bonding and, within experimental error, are identical to those of the corresponding "ate" complexes. Similar to **9a** and **9d**, the sum of the bond angles about boron in **10a** and **10d** is 360°, although the geometry is distorted from trigonal. Additionally, the N1−Ln−N2 angle is slightly larger in both cases (by approximately 1.5°) when compared to **9a**

(33) Dutton, J. L.; Sutrisno, A.; Schurko, R. W.; Ragogna, P. J. *Dalton Trans.* **2008**, 3470.

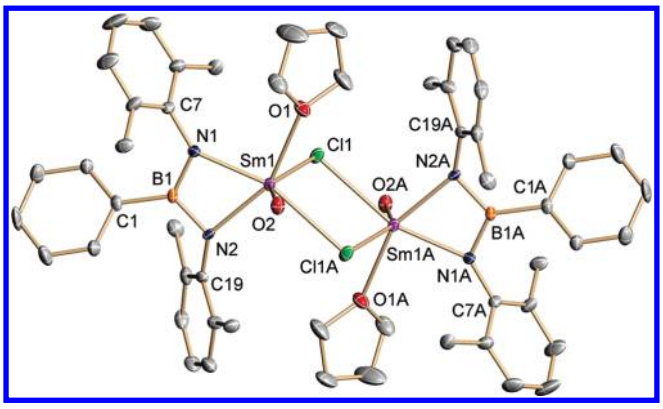

Figure 3. Molecular structure of **10d** (representative of **10a**). Hydrogen atoms are omitted, and only the α-carbon atoms of Dipp groups and the O atoms of one of the THF molecules are shown for clarity. Symmetry elements used to generate equivalent atoms: #1 $-x,-y+3,-z+1$.

Table 4. Crystallographic Data for **10a** and **10d**

empirical formula	$C_{38}H_{55}BClN_2O_2Y$	$C_{38}H_{55}BClN_2O_2Sm$
fw	707.01	768.45
cryst. system	monoclinic	monoclinic
space group	$P2(1)/n$	$P2(1)/n$
a, Å	13.690(3)	13.825(3)
b, Å	15.867(3)	15.955(3)
c, Å	18.516(4)	18.451(4)
α, deg.	90.00	90.00
β, deg.	93.24(3)	94.06(3)
γ, deg.	90.00	90.00
V, Å^3	4016(1)	4056(1)
Z	4	4
T, °C	−100	−100
ρ_{calcd}, g/cm^3	1.169	1.257
μ(Mo Kα), mm^{-1}	1.550	1.543
crystal size, mm^3	0.16 × 0.14 × 0.08	0.20 × 0.16 × 0.10
F(000)	1496	1588
Θ range, deg	2.55−25.02	2.56−25.03
reflns collected	51912	54928
unique reflns	7069	7149
R_{int}	0.1061	0.1056
R_1 [$I > 2\sigma(I)$][b]	0.0661	0.0565
wR_2 (all data)[c]	0.1401	0.1184
GOF on F^2	1.077	1.060
completeness	0.997	0.998

and **9d**. The geometry about the lanthanide center is greatly distorted from octahedral, as observed for the "ate" complexes, with bond angles ranging from approximately 65° to 155°. In both **10a** and **10d** the Ln−Cl1 bond length is slightly shorter and Ln−Cl1A is slightly longer than the corresponding distances in **9a** and **9d**; however, both distances still fall in the expected range for a bridging Y−Cl and Sm−Cl bond. The asymmetry in the chloride bridging is more pronounced in **10a** and **10d** than in the "ate" complexes, with the difference in the two Ln−Cl bond lengths being approximately 0.1 Å. As observed for samarium "ate" complex **9d**, the ^{1}H NMR spectrum could be obtained for the neutral complex **10d**, despite it being paramagnetic. A similar degree of deshielding of aryl resonances and shielding of alkyl resonances to that noticed for **9d** is found, and all signals are significantly broadened because of the paramagnetic samarium(III) center.

Table 5. Selected Bond Lengths (Å) and Bond Angles (deg) for *bam*LnCl(THF)$_2$, **10a** and **10d**

	10a (Y)	**10d (Sm)**
B1−N1	1.447(6)	1.443(8)
B1−N2	1.451(6)	1.468(8)
N1−Ln	2.218(4)	2.266(5)
N2−Ln	2.204(4)	2.250(5)
Cl1−Ln	2.684(1)	2.749(2)
Cl1A−Ln	2.781(1)	2.846(2)
N1−B1−N2	112.8(4)	112.4(5)
N1−B1−C1	124.0(4)	124.6(5)
N2−B1−C1	123.1(4)	123.0(6)
C7−N1−B1	125.0(4)	124.7(5)
C7−N1−Ln	144.6(3)	143.7(4)
B1−N1−Ln	90.3(3)	91.4(3)
C19−N2−B1	125.9(4)	126.1(5)
C19−N2−Ln	140.3(3)	139.1(4)
B1−N2−Ln	90.7(3)	91.4(3)
N2−Ln−N1	66.2(1)	64.7(2)
N2−Ln−O2	99.6(1)	101.2(2)
N1−Ln−O2	98.7(1)	98.4(2)
N2−Ln−O1	155.2(1)	153.3(2)
N1−Ln−O1	89.8(1)	89.1(2)
O2−Ln−O1	77.4(1)	76.0(2)
N2−Ln−Cl1	106.2(1)	107.1(1)
N1−Ln−Cl1	109.4(1)	110.6(1)
O2−Ln−Cl1	147.6(1)	146.0(1)
O1−Ln−Cl1	86.7(1)	86.7(1)

Conclusion

We have synthesized and structurally characterized the first examples of lanthanide complexes containing a dianionic boraamidinate ligand, {[Li(THF)$_4$][*bam*LnCl$_2$(THF)]}$_2$ (Ln = Y, Pr, Nd, Sm, Ho, Er, Yb).[28] All seven complexes are isostructural, forming dimers in the solid state through bridging chlorides. Proton NMR spectra were obtained for paramagnetic complexes Ln = Pr, Nd, Sm and show a shift induced by the lanthanide center in both the aryl (deshielded) and the alkyl (shielded) regions. The treatment of {[Li(THF)$_4$][*bam*LnCl$_2$(THF)]}$_2$ (Ln = Y, Sm) with an excess of TMSOTf produced *bam*LnCl(THF)$_2$, which is also dimeric in the solid state. Preliminary investigations have shown that the reactions of {*bam*SmCl(THF)$_2$}$_2$ with lithium or potassium bis(trimethylsilyl)amide and with lithium diisopropylamide (LDA) do not proceed cleanly. Consequently, our current focus is on the use of the corresponding iodides for metathetical reactions.

Acknowledgment. The authors thank the Natural Sciences and Engineering Council (Canada) and the Alberta Ingenuity Fund (A.M.C.) for financial support. We also gratefully acknowledge Prof. Dr. Sjoerd Harder for regular correspondence informing us of his results with related lanthanide complexes of the *bam* ligand [HB(NDipp)$_2$]$^{2-}$ and for his helpful advice.

Supporting Information Available: X-ray crystallographic files in CIF format. This material is available free of charge via the Internet at http://pubs.acs.org.